Physics Laboratory 2 for Beginners
Laboratory in Winter Semester 2018/19

Experiment 83: Bragg reflection of X-Rays on a Monocrystal

(carried out on 29. March 2019 under supervision of [redacted])

[redacted]

1. April 2019

Contents

Table 1 shows an overview of the symbols used in this lab report.

Symbol	Meaning
a	Size of a unit cell from a crystal
α	Bragg angle
α_{min}	Minimal Bragg angle
α_{x}	Bragg angle for a specific line K
d	Lattice constant
h	Planck constant
$\nu_{\text{K}x}$	Frequency of a specific line K$_x$
ν_{max}	Maximal frequency
λ	Wavelength
λ_{min}	Minimal wavelength
$\lambda_{\text{K}x}$	Wavelength of a specific line K$_x$
U	Voltage
U_{A}	Anode voltage
U_{Z}	Counter voltage
Ry	Rydberg Constant
e	Elementary charge
c_0	Speed of light
s_x	Error on the (measured) quantity x
x_{lit}	Literature value of the quantity x
x_{calc}	Calculated value of quantity x
Z	atomic number of an element

Table 1: Symbols used in this lab report

1 Objective

In this experiment we first have to record the characteristic of a Geiger-Müller counter. Afterwards we have to measure the bremsstrahlung spectrum together with the K$_\alpha$- and the K$_\beta$-X-rays of a copper diode by using a monocrystal. Furthermore we have to calculate the lattice constant, the wavelength of the Cu K_β-line and the wavelength of the Cu K_α-radiation. In the end we have to determine the Planck constant.

2 Theoretical Basis

X-Rays are generated when electrons are accelerated or decelerated and electromagnetic radiation is emitted during the process. If an electron is accelerated by traversing a voltage difference U_{A} it gains kinetic energy $E_{\text{kin}} = e \cdot U_{\text{A}}$. If the kinetic energy is fully converted to a quantum, the energy balance

$$h\nu_{\text{max}} = \frac{hc_0}{\lambda_{\text{min}}} = e \cdot U_{\text{A}}. \tag{1}$$

holds, where ν_{max} is the maximal frequency of the bremsstrahlung spectrum. Bremsstrahlung occurs when electrons are accelerated towards an anti cath-

ode and interact with the coulomb field of the nucleus of the atoms making up the anti cathode.

So called K_α-X-Rays are generated when accelerated electrons hit the inner electrons of the nuclei of the anti cathode material and knock them away from their nuclei so that an electron from the L-shell has to fill the emerging hole. To determine the frequency (or equivalently: the wavelength) of the emitted K_α-X-Rays one can use the law of Moseley:

$$\nu_{K_\alpha} = \frac{c_0}{\lambda_{K_\alpha}} = \frac{3}{4}(Z-1)^2 \mathrm{Ry} \tag{2}$$

$\mathrm{Ry} = 3.290 \times 10^{15}\,\mathrm{Hz}$ is the so called rydberg frequency and Z stands for the atomic number of the cathode nucleus. The characteristic line spectrum of the X-rays results out of the ionisation of some atoms when electrons arrive at the cathode.

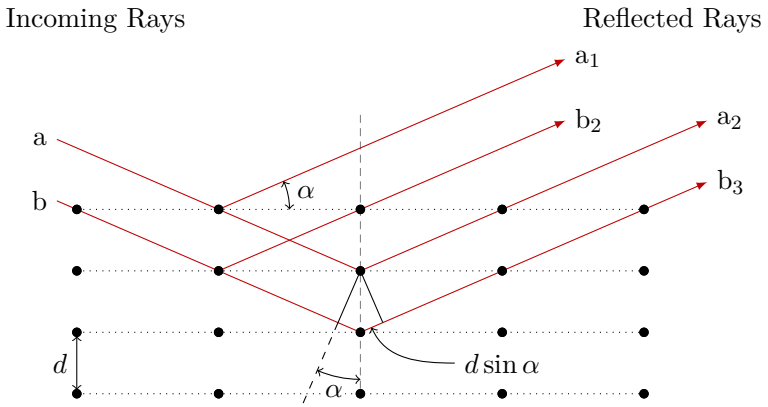

Figure 1: Bragg reflection of X-Ray radiation

Now we will shortly explain how the Bragg reflection works: In a mono crystal one can find different lattice planes (cf. fig. 1). When X-rays arrive at a mono crystal, they get scattered in many different directions. If the path difference of two adjacent rays arriving in different lattice planes in the mono crystal is a multiple of the radiations wavelength λ, constructive interference occurs. This can be expressed mathematically in the following way:

$$2d \sin\alpha = n\lambda. \tag{3}$$

It means that it comes to constructive interference between two rays which are reflected on different lattice planes of a crystal when their path difference is $2d \sin\alpha$. d is the distance between the lattice planes and α is the angle of incidence of the radiation. Rays which are reflected by the same lattice plane don't show any path difference. Figure 2 shows a schematic overview over the atomic geometry of the crystal we used in our measurements. The

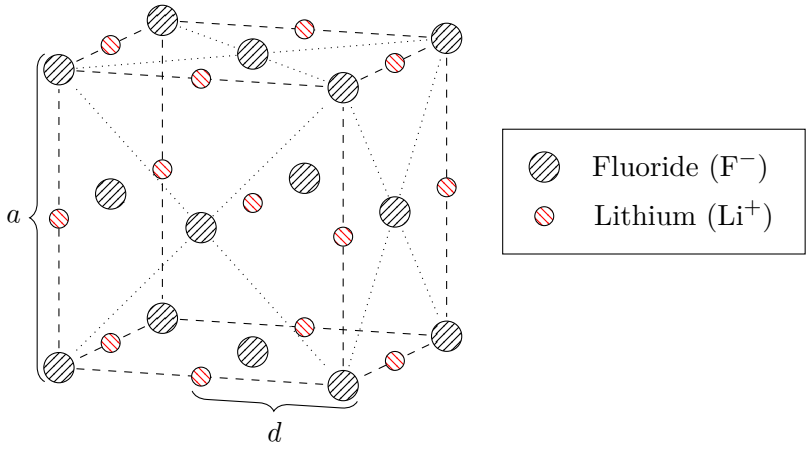

Figure 2: Geometry of a Lithium-Fluoride crystal. Depicted is a single unit cell.

atomic structure suggests that the lattice constant d, which is also shown in fig. 1, is related to the unit cell size a of the crystal by

$$a = 2d. \tag{4}$$

3 Setup and Procedure

For our measurements we used an X-ray device with a radiation detector which in turn was connected to a discriminator feeding into a counting device. In the X-ray device one can find an X-ray tube and a crystal on a swiveling vertical axis. One can also find a radiation detector, which can swivel around the crystal. During the measurement we had to control the voltage U_A of the anode. The detector was connected to an external high-voltage device. By use of a cord the signals picked up by the detector could get to the counting device. With these counts we could determine the outline of the spectrum of the reflected radiation for a constant time of counting for different angles.

In order to determine the characteristic of the counter, we measured the number of the pulses for a specific time (30 s each) for multiple values of the voltage U_Z of the counter. The distance between two adjacent voltage values was adjusted according to the increase of counted signals.

We investigated the X-ray emission spectrum in three different ways:

In order to get an overview of the whole spectrum and investigate the rough position of the extrema, we noted the number of registered pulses N for a constant counter voltage in a specific time of counting depending on the Bragg angle α.

Afterwards we had a close look on the maximum values of the spectrum

and on how the shape in the position of the maximums from the characteristic lines change for small changes of the Bragg angle, which we adjusted in small steps. We realized this measurement by measuring the registered signals for small changes of the angle in the area of the maximums.

In addition we took this measurement in the area with small angles to investigate the beginning of the continuum.

4 Measurement

For all our measurements we used a LiF-monocrystal with an interplanar distance of 201 pm.

4.1 Charakteristic of the Counter

First we adjusted the voltage of the anode to a value of 20 kV, the angle of Bragg reflection to a value of 12° and the counting time to a value of 30 s.

In order to measure the characteristic of the counter, we measured the number of pulses in 30 s dependent on the voltage U_Z of the counter. The value of this voltage we changed in steps of 25 V between 300 V to 850 V. In the interesting area of measuring, i. e. when we detected a great increase in counts, we chose a smaller stepwidth. For the error on the counted numbers of registered signals the square root of the registered number was chosen. We justify this by approximating the distribution of the measured counts with a poisson distribution from which the variance can be estimated by the arithmetic mean of all given observations (in our case our only observation is N), meaning that the standard deviation of a poisson distributed random variable can be estimated by taking the square root of the estimator of the variance, i. e. the mean.

For the voltage of the counter we decided to take an uncertainty of 0.5 V as the number of shown digits on the display for the voltage was limited, so that the smallest possible measureable value was 1 V. One can see the results of our measurements in table 2.

4.2 Spectrum of X-Ray Emission

In order to investigate the whole spectrum we measured the number of registered pulses depending on the Bragg angle for a constant counter voltage U_Z of 500 V in a counting time of 15 s. For the counting time we chose a value of 15 s, as we were able to detect 2000 signals at a Bragg angle of 12° for this counting time, as was suggested in the manual [3]. The results from our measurements are shown in table 3.

Afterwards we repeated the measurement for a stepwidth of 0.2° in the area of the maximal value of registered signals. Because of the previous

experience our assistant had with this experiment we took this measurement two times. One can see our results in table 4.

After that we conducted the same measurement as described above for the minimum of the spectrum. For the same reasons as before we decided to take this measurement two times. Because the results didn't seem to be compatible, we took the same series of measurement a third time. One can find our results in table 5.

All the measurements we took during the experiment can be found in the appendix.

5 Analysis

5.1 Characteristic of the Counter

In order to analyse the characteristic of the counter, we plotted our measurements from table 2 in the graph shown in fig. 3. As expected, a rapid increase in events followed by a long plateau could be observed.

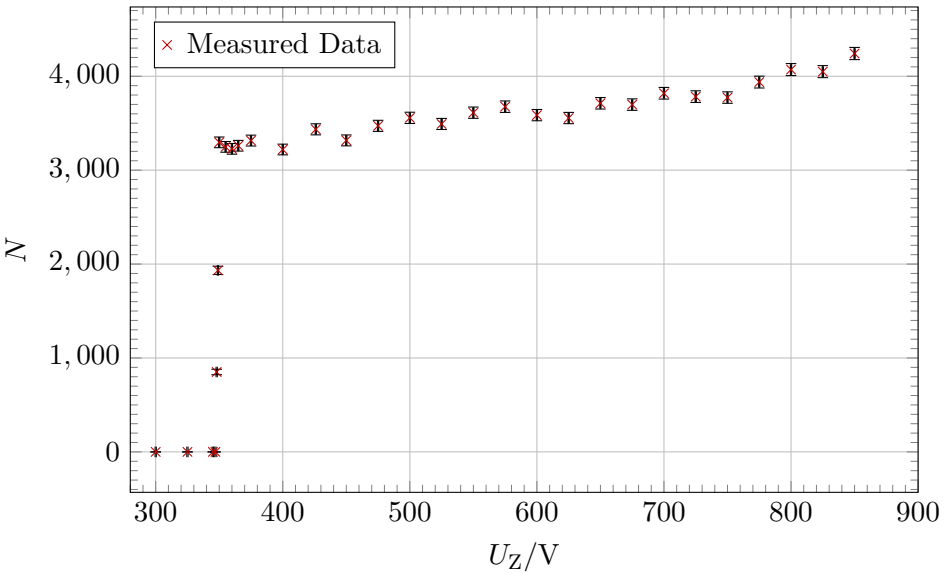

Figure 3: Characteristic of the Counter: The counted events N from table 2 is plotted against the counter voltage U_Z in order to find the optimal voltage for further measurements.

5.2 Determination of the Lattice Constant

Out of the results from our two measurements for the number of registered signals N against the Bragg angle α, which one can see in section 4.2 we

created three graphs based on the measurements given in tables 3 to 5. In fig. 4, which is based on table 3, one can see the whole spectrum while fig. 5 shows the three measurements of counting rate for small angles.

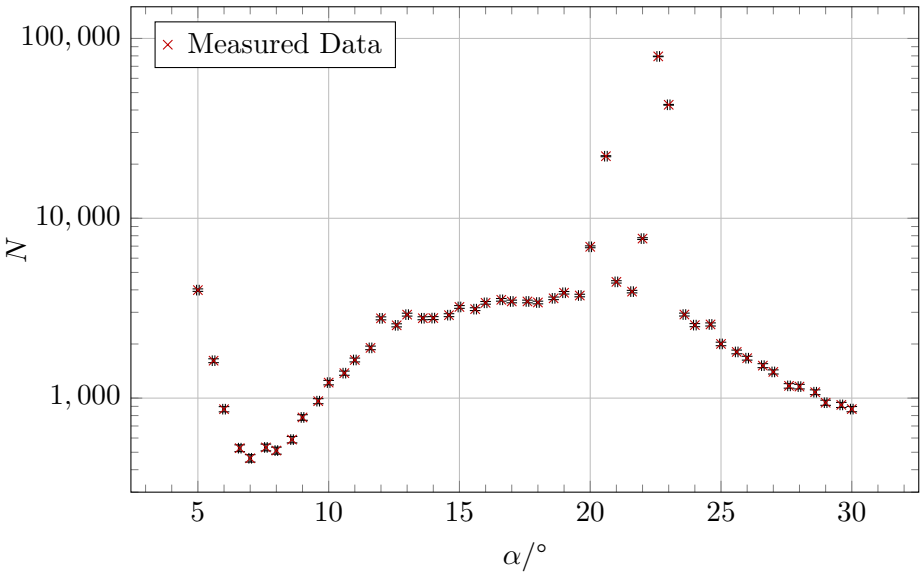

Figure 4: Complete Spectrum of the number of registered signals against the Bragg angle α

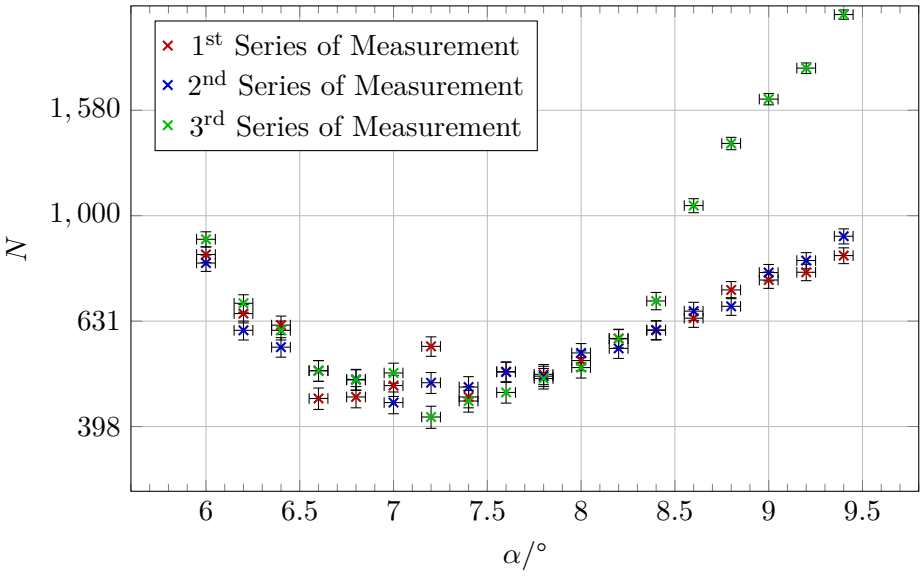

Figure 5: number of registered signals against the Bragg angle α for small angles on logarithmic scale

The plot fig. 6 shows the number of counts against the Bragg angle in the area of the maximal value of registered signals. The graph contains both measurement series from table 4.

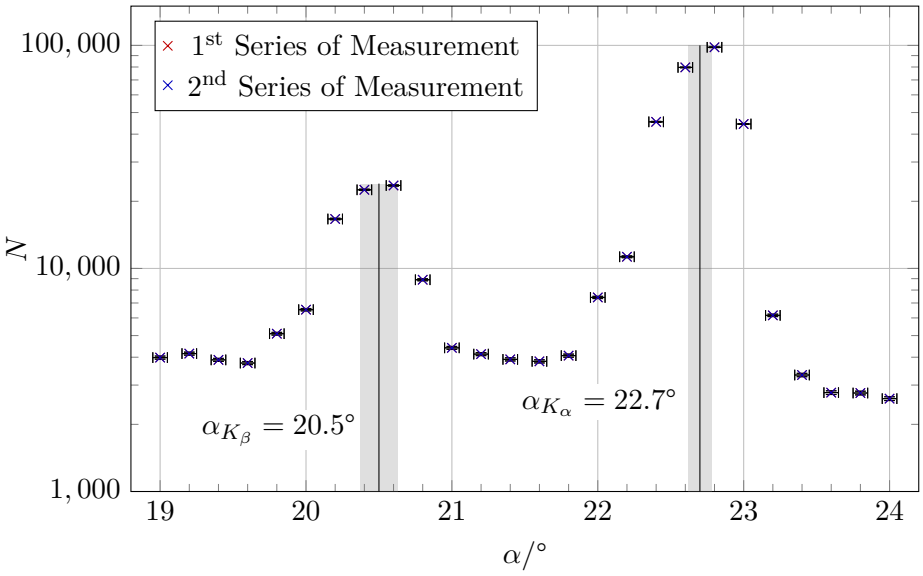

Figure 6: number of registered signals against the Bragg angle α near the maximums

Because the overall values of both measurement series don't differ too much we could estimate the Bragg angle for the highest number of registered signals with great confidence. The angle at which the count rate is at a maximum is marked alongside the measurements in fig. 6. We estimated the Bragg angle at a value of

$$\alpha_{\mathrm{K}_\alpha} = (22.70 \pm 0.08)°. \tag{5}$$

The error on this value has been manually estimated by us by looking at the distance between the two maximum points.

Now the lattice constant can be calculated by use of eq. (3):

$$d = \frac{\lambda}{\sin \alpha_{\mathrm{K}_\alpha}} = 199.9\,\mathrm{pm} \tag{6}$$

Because we only took measurements of the first peak, k has to equal one. The wavelength $\lambda = 154.2\,\mathrm{pm}$ was extracted from the manual [3]. By use of Gaussian error propagation one can estimate the error on the lattice constant:

$$s_d = s_{\alpha_{\mathrm{K}_\alpha}} \frac{\lambda \cos \alpha_{\mathrm{K}_\alpha}}{2 \sin^2(\alpha_{\mathrm{K}_\alpha})} = 1.0\,\mathrm{pm}. \tag{7}$$

Therefore we obtain a value of the lattice constant of:

$$d = (199.9 \pm 0.7)\,\mathrm{pm}. \tag{8}$$

Using the lattice constant and eq. (4) one can calculate the size a of a crystal unit cell as

$$a = 2d = 399.8\,\mathrm{pm} \tag{9}$$

with an error of

$$s_a = 2s_d = 1.4\,\mathrm{pm}. \tag{10}$$

5.3 Calculation from the Wavelengths of the K_α- and the K_β-line

By looking at fig. 6 we can estimate the Bragg angle for which the count rate becomes maximum for the first time, which corresponds to the K_β-line. By estimation, one arrives at

$$\alpha_{K_\beta} = (20.50 \pm 0.13)^\circ. \tag{11}$$

By looking again at the distance between the two highest measured values of the counting rate we estimated the uncertainty of the angle. As the distance between these two points seems a bit higher for the K_β-line than for the K_α-line, we estimated a higher error for the angle of the K_β-line than for the K_α-line accordingly.

With the priorly calculated value of the lattice constant d we can now calculate the wavelength of the K_β-line. This can be achieved by use of Equation (3). As a result we obtain:

$$\lambda_{K_\beta} = 2d \sin \alpha_{K_\beta} = 140.0\,\mathrm{pm}. \tag{12}$$

The error on the wavelength can once again be obtained by the use of Gaussian error propagation:

$$s_{\lambda_{K_\beta}} = \sqrt{\left(s_d 2 \sin \alpha_{K_\beta}\right)^2 + \left(s_\alpha 2d \cos \alpha_{K_\beta}\right)^2} = 0.9\,\mathrm{pm}. \tag{13}$$

The wavelength of the K_β-line is thus $(140.0 \pm 0.9)\,\mathrm{pm}$.

In addition one can calculate the wavelength of the K_α-line in good approximation by the law of Moseley eq. (2). First we calculate the frequency of the K_α-line. The atomic number of copper is $Z = 29$. With the Rydberg-frequency we get a frequency of

$$\nu_{K_\alpha} = \frac{3}{4}(Z-1)^2 \mathrm{Ry} = 1.93 \times 10^{18}\,\mathrm{Hz}. \tag{14}$$

With this value the wavelength can be calculated:

$$\lambda_{K_\alpha} = \frac{c_0}{\nu_{K_\alpha}} = 155.1\,\mathrm{pm}. \tag{15}$$

5.4 Use of Bremsstrahlung and Determination of the Plack Constant

Figure 7 shows a graph based on our measurements given in table 5. By graphical estimation of the angle $\alpha_{\min}$ for which the spectrum approaches a local minimum one can approximate the point at which bremsstrahlung occurs:

$$\alpha_{\min} = (7.3 \pm 1.3)^\circ. \tag{16}$$

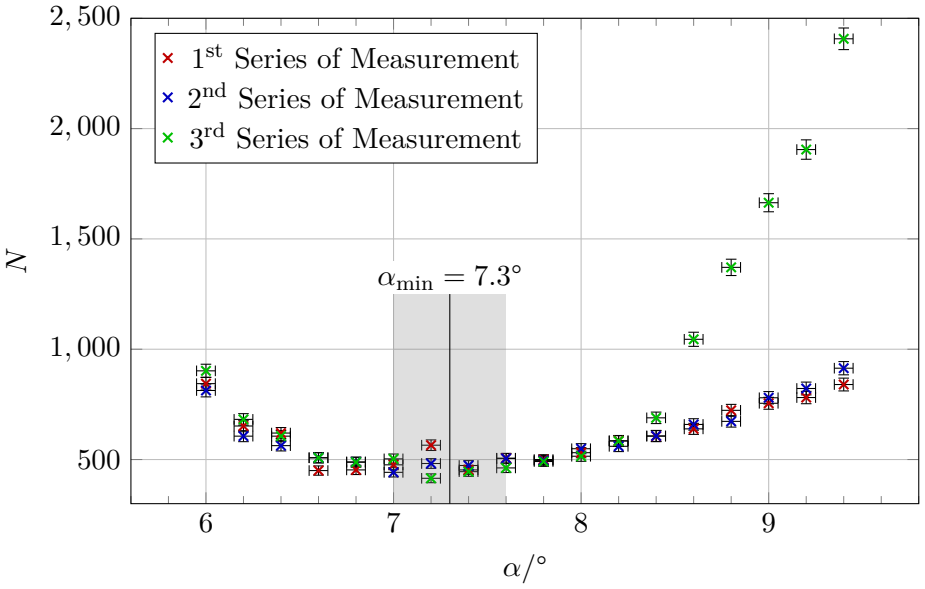

Figure 7: number of registered signals against the Bragg angle α for small angles

The error on this angle was estimated alongside the angle itself. As the three measurement series differ quite a lot, we have to admit that the best value of the angle isn't really exact. We tried to counter this by choosing the margin of error to be an unusually high value.

With $\alpha_{\min}$ we can calculate by use of eq. (3) the minimum wavelength $\lambda_{\min}$:

$$\lambda_{\min} = 2d \sin \alpha_{\min} = 51\,\mathrm{pm} \tag{17}$$

For d we used the value which we calculated prior for the lattice constant in eq. (8). We determined the error on the wavelength by use of Gaussian error propagation:

$$s_{\lambda_{\min}} = \sqrt{(s_d 2 \sin \alpha_{\min})^2 + (s_{\alpha_{\min}} 2d \cos \alpha_{\min})^2} = 2\,\mathrm{pm}. \tag{18}$$

By use of eq. (1) one can now calculate the Planck constant h:

$$h = \frac{e \cdot U_\mathrm{A}}{c_0} \lambda_\mathrm{min} = 6.00\,\mathrm{J\,s} \tag{19}$$

The speed of light[1] c_0 as well as the elementary charge[2] e was assumed to be exact [1]. The error on h can once again be determined by use of Gaussian error propagation:

$$s_h = \frac{e \cdot U_\mathrm{A}}{c_0} s_{\lambda_\mathrm{min}} = 0.20\,\mathrm{J\,s}. \tag{20}$$

Thus, our result for the Planck constant becomes

$$h = (6.00 \pm 0.20) \times 10^{-34}\,\mathrm{Js}. \tag{21}$$

6 Discussion

6.1 Characteristic of the Counter

In fig. 3 one can see the characteristic of the counter. We remarked a rapid increase in events followed by a long plateau.

By looking at fig. 3 one can also see that the measured points fluctuate quite visibly. In addition the number of registered events still increases after reaching the plateau. This could have been caused because it was the first one of our measurements so that the high voltage generator hasn't had enough time to heat, which results in the voltage not having enough time to steady itself. That would also explain why the counting rate in this measurement series is all in all lower than in all the following experiments (the difference of the counting rates between the experiments is so high that it couldn't have been caused by a difference in 2 kV of the anode voltage).

Even so the beginning of the plateau is well visible in the diagram. Although one can't clearly see at which point the plateau ends, we estimate the middle of the plateau at a voltage of around 500 V as it looks like the plateau begins at a voltage of around 400 V and ends at a voltage of around 600 V, at which point the number of measured events increases again.

6.2 Graphical Observation of the Spectrum

In fig. 4 one can see the whole spectrum of the measured points from the counting against the adjusted angle α. It gets obvious that there are two points of maximal value corresponding to the expected K_α- and K_β-line.

[1] $c_0 = 299\,792\,458\,\frac{\mathrm{m}}{\mathrm{s}}$.
[2] $e = 1.602 \times 10^{-19}\,\mathrm{C}$

Additionally the underlying bremsstrahlung spectrum sets in before the first K_β-peak and steadily declines beyond it.

Figure 6 shows the course of the spectrum near the maximums in detail. We can see that we have two local maxima which are clearly separated by a few points inbetween. We estimated that we have one maximum at an angle of

$$\alpha_{K_\alpha} = (22.70 \pm 0.08)^\circ. \tag{22}$$

This belongs to the K-α-line. We also estimated the maximum of the K-β-line to be at an angle of

$$\alpha_{K_\beta} = (20.50 \pm 0.13)^\circ. \tag{23}$$

Figure 5 shows the minimum of the spectrum for small angles in detail. First one can say that the difference between the values of the three measurements is relatively high. That may be caused by a systematic error from the set-up of our experiment as our assistant said before.

In the diagram one can also see that the counting rate for small angles is relatively high. This is the result of some of the X-rays passing directly into the detector without having been reflected on the crystal lattice planes. We estimated the minimum at an angle of

$$\alpha_{\min} = (7.3 \pm 0.3)^\circ, \tag{24}$$

as it is shown in fig. 7. This corresponds to the point where the continuous spectrum begins and bremsstrahlung sets in.

6.3 Determination of the Lattice Constant

By use of the angle we estimated for the K-α-line before we were able to calculate the lattice constant:

$$d_{\text{calc}} = (199.9 \pm 0.7)\,\text{pm}. \tag{25}$$

According to the label on the LiF-crystal that we used in our measurements, the lattice constant equals

$$d = 201\,\text{pm}. \tag{26}$$

The calculated value of the lattice constant exists in a 1.5σ-environment of the expected value for the lattice constant. Because of that we can say we obtained a good result from our measurement within reasonable margins of uncertainty.

By using the result for the lattice constant we easily calculated the size of a unit cell to be

$$a_{\text{calc}} = (399.8 \pm 1.4)\,\text{pm}. \tag{27}$$

6.4 Calculation from the Wavelengths of the K_α- and the K_β-line

With the already calculated value of the lattice constant we could determine the wavelength of the K_β-line:

$$\lambda_{K,\beta_{calc}} = (140.0 \pm 0.9)\,\text{pm}. \tag{28}$$

The literature value [2] for this characteristic line is

$$\lambda_{K,\beta_{lit}} = (139.223\,40 \pm 0.000\,60)\,\text{pm}. \tag{29}$$

It is obvious that our calculated value of the wavelength corresponds with the literature value, because the literature value is in a one σ-environment of the calculated value. By use of the law of Moseley we also calculated the wavelength of the K_α-line. As a result we obtained:

$$\lambda_{K,\alpha_{calc}} = \frac{c}{\nu_{K,\alpha}} = 155.1\,\text{pm}. \tag{30}$$

The calculated value corresponds relative good with the value of the wavelength from the K_α-line given in [3]:

$$\lambda_{K,\alpha_{lit}} = \frac{c}{\nu_{K,\alpha}} = 154.2\,\text{pm}. \tag{31}$$

The difference between these values could be caused, because we used the approximately value of $c = 3 \times 10^8\,\text{m/s}$ and not the exact value of the speed of light for our calculation.

6.5 Use of Bremsstrahlung and Calculation of the Planck Constant

By looking at fig. 7 we estimated the angle α_{min} at which bremsstrahlung occurs:

$$\alpha_{min} = (7.3 \pm 1.3)^\circ. \tag{32}$$

Then we calculated the minimal wavelength λ_{min} by using the condition of Bragg:

$$\lambda_{min} = 2d \sin \alpha_{min} = (51 \pm 2)\,\text{pm} \tag{33}$$

With this result we obtained for the Planck constant h:

$$h_{calc} = (6.00 \pm 0.20) \times 10^{-34}\,\text{J s} \tag{34}$$

The literature value [1] of the constant is:

$$h_{lit} = 6.626\,\text{Js}. \tag{35}$$

It's clear to see that our calculated value for the Planck constant is within around 3σ-environments of the literature value. The deviation between these values may result out of a systematic error: As one can see in fig. 7 it wasn't easy to estimate the exact point where the minimal value of the Bragg angle is located. It could be located everywhere between 6.5° to 8°. Because the point is so difficult to determine, we already chose a high uncertainty for the estimated value of the minimal Bragg angle α_{min}. Out of the value we calculated for the Planck constant it gets obvious that we should have estimated a higher value of α_{min} and probably a higher uncertainty on it. That would result in a higher value for λ_{min} which would again result in an higher calculated value for the Planck constant. Another cause for the high deviation between the three measurements in table 5 and fig. 7 may be that we accidentally switched off the counter voltage U_{Z} between the first two measurements. Although the measurements in table 3 were unaffected, we can't say with clarity that this didn't cause the high deviation of our data from table 5. Another point to consider is the failure rate of the counter. While the probability of not measuring an event should stay the same throughout all measurements, outside factors such as temperature or humidity may greatly impact the discriminators function.

In addition there could have been another systematic error in our measurements, because in the area of small Bragg angles occurs scattered radiation which increases the number of registered pulses. This again results in a shift of the value from the Bragg angle to smaller angles. Although this argument can be supported using the relatively old machinery supporting the alignment of the crystal and the detector, the data in fig. 7 shows that especially the third measurement features a much greater increase than we would expect from a simple offset.

Respecting these systematic errors, we can say the value we calculated for the Planck constant is abrasively compatible with the literature value all in all.

A Appendix

A.1 Measured Values

U_Z in V	N	U_Z in V	N
300.0 ± 0.5	0 ± 1	500.0 ± 0.5	3560 ± 60
325.0 ± 0.5	0 ± 1	525.0 ± 0.5	3490 ± 60
345.0 ± 0.5	0 ± 1	550.0 ± 0.5	3610 ± 60
347.0 ± 0.5	0 ± 1	575.0 ± 0.5	3680 ± 60
348.0 ± 0.5	851 ± 29	600.0 ± 0.5	3590 ± 60
349.0 ± 0.5	1930 ± 40	625.0 ± 0.5	3560 ± 60
350.0 ± 0.5	3300 ± 60	650.0 ± 0.5	3710 ± 60
355.0 ± 0.5	3250 ± 60	675.0 ± 0.5	3700 ± 60
360.0 ± 0.5	3230 ± 60	700.0 ± 0.5	3820 ± 60
365.0 ± 0.5	3260 ± 60	725.0 ± 0.5	3780 ± 60
375.0 ± 0.5	3320 ± 60	750.0 ± 0.5	3770 ± 60
400.0 ± 0.5	3220 ± 60	775.0 ± 0.5	3940 ± 60
426.0 ± 0.5	3440 ± 60	800.0 ± 0.5	4070 ± 60
450.0 ± 0.5	3320 ± 60	825.0 ± 0.5	4050 ± 60
475.0 ± 0.5	3470 ± 60	850.0 ± 0.5	4240 ± 70

Table 2: Characteristic of the counting device (cf. section 4.1)

α in °	N	α in °	N
5.0 ± 0.1	3990 ± 60	18.0 ± 0.1	3400 ± 60
5.6 ± 0.1	1620 ± 40	18.6 ± 0.1	3590 ± 60
6.0 ± 0.1	868 ± 29	19.0 ± 0.1	3850 ± 60
6.6 ± 0.1	527 ± 23	19.6 ± 0.1	3720 ± 60
7.0 ± 0.1	463 ± 22	20.0 ± 0.1	6940 ± 80
7.6 ± 0.1	532 ± 23	20.6 ± 0.1	$22\,140 \pm 150$
8.0 ± 0.1	511 ± 23	21.0 ± 0.1	4430 ± 70
8.6 ± 0.1	588 ± 24	21.6 ± 0.1	3910 ± 60
9.0 ± 0.1	781 ± 28	22.0 ± 0.1	7710 ± 90
9.6 ± 0.1	960 ± 30	22.6 ± 0.1	$79\,460 \pm 280$
10.0 ± 0.1	1220 ± 30	23.0 ± 0.1	$42\,770 \pm 210$
10.6 ± 0.1	1380 ± 40	23.6 ± 0.1	2920 ± 50
11.0 ± 0.1	1630 ± 40	24.0 ± 0.1	2550 ± 50
11.6 ± 0.1	1900 ± 40	24.6 ± 0.1	2570 ± 50
12.0 ± 0.1	2780 ± 50	25.0 ± 0.1	2000 ± 40
12.6 ± 0.1	2540 ± 50	25.6 ± 0.1	1810 ± 40
13.0 ± 0.1	2910 ± 50	26.0 ± 0.1	1670 ± 40
13.6 ± 0.1	2780 ± 50	26.6 ± 0.1	1520 ± 40
14.0 ± 0.1	2790 ± 50	27.0 ± 0.1	1400 ± 40
14.6 ± 0.1	2890 ± 50	27.6 ± 0.1	1170 ± 30
15.0 ± 0.1	3210 ± 60	28.0 ± 0.1	1160 ± 30
15.6 ± 0.1	3120 ± 60	28.6 ± 0.1	1080 ± 30
16.0 ± 0.1	3390 ± 60	29.0 ± 0.1	940 ± 30
16.6 ± 0.1	3520 ± 60	29.6 ± 0.1	920 ± 30
17.0 ± 0.1	3450 ± 60	30.0 ± 0.1	869 ± 29
17.6 ± 0.1	3450 ± 60		

Table 3: Counted events N measured with respect to the bragg angle α within the scope of section 4.2.

	N	
α in °	1st Measurement	2nd Measurement
19.0 ± 0.1	3980 ± 60	3800 ± 60
19.2 ± 0.1	4150 ± 60	3930 ± 60
19.4 ± 0.1	3890 ± 60	3850 ± 60
19.6 ± 0.1	3770 ± 60	3770 ± 60
19.8 ± 0.1	5100 ± 70	5030 ± 70
20.0 ± 0.1	6530 ± 80	6670 ± 80
20.2 ± 0.1	$16\,660 \pm 130$	$16\,550 \pm 130$
20.4 ± 0.1	$22\,520 \pm 150$	$22\,380 \pm 150$
20.6 ± 0.1	$23\,550 \pm 150$	$23\,190 \pm 150$
20.8 ± 0.1	8900 ± 90	8780 ± 90
21.0 ± 0.1	4410 ± 70	4470 ± 70
21.2 ± 0.1	4130 ± 60	4110 ± 60
21.4 ± 0.1	3910 ± 60	4020 ± 60
21.6 ± 0.1	3830 ± 60	3870 ± 60
21.8 ± 0.1	4070 ± 60	4080 ± 60
22.0 ± 0.1	7420 ± 90	7600 ± 90
22.2 ± 0.1	$11\,280 \pm 110$	$11\,280 \pm 110$
22.4 ± 0.1	$45\,420 \pm 210$	$46\,350 \pm 220$
22.6 ± 0.1	$79\,670 \pm 280$	$78\,970 \pm 280$
22.8 ± 0.1	$98\,100 \pm 300$	$97\,600 \pm 300$
23.0 ± 0.1	$44\,420 \pm 210$	$43\,080 \pm 210$
23.2 ± 0.1	6160 ± 80	6290 ± 80
23.4 ± 0.1	3330 ± 60	3300 ± 60
23.6 ± 0.1	2780 ± 50	2820 ± 50
23.8 ± 0.1	2760 ± 50	2730 ± 50
24.0 ± 0.1	2610 ± 50	2510 ± 50

Table 4: Counted events N measured with respect to the bragg angle α near K_α and K_β lines in the intensity spectrum

	N		
α in °	1^{st} Measurement	2^{nd} Measurement	3^{rd} Measurement
6.0 ± 0.1	844 ± 29	813 ± 29	900 ± 30
6.2 ± 0.1	652 ± 26	606 ± 25	682 ± 26
6.4 ± 0.1	620 ± 25	563 ± 24	606 ± 25
6.6 ± 0.1	450 ± 21	508 ± 23	508 ± 23
6.8 ± 0.1	453 ± 21	489 ± 22	488 ± 22
7.0 ± 0.1	476 ± 22	442 ± 21	503 ± 22
7.2 ± 0.1	565 ± 24	482 ± 22	415 ± 20
7.4 ± 0.1	453 ± 21	473 ± 22	445 ± 21
7.6 ± 0.1	506 ± 22	505 ± 22	462 ± 21
7.8 ± 0.1	500 ± 22	496 ± 22	491 ± 22
8.0 ± 0.1	531 ± 23	549 ± 23	515 ± 23
8.2 ± 0.1	585 ± 24	560 ± 24	584 ± 24
8.4 ± 0.1	606 ± 25	607 ± 25	689 ± 26
8.6 ± 0.1	639 ± 25	659 ± 26	1040 ± 30
8.8 ± 0.1	723 ± 27	673 ± 26	1370 ± 40
9.0 ± 0.1	755 ± 27	780 ± 28	1660 ± 40
9.2 ± 0.1	781 ± 28	822 ± 29	1900 ± 40
9.4 ± 0.1	840 ± 29	910 ± 30	2410 ± 50

Table 5: Counted events N measured with respect to the bragg angle α near the beginning of bremsstrahlung

A.2 Lab Notes

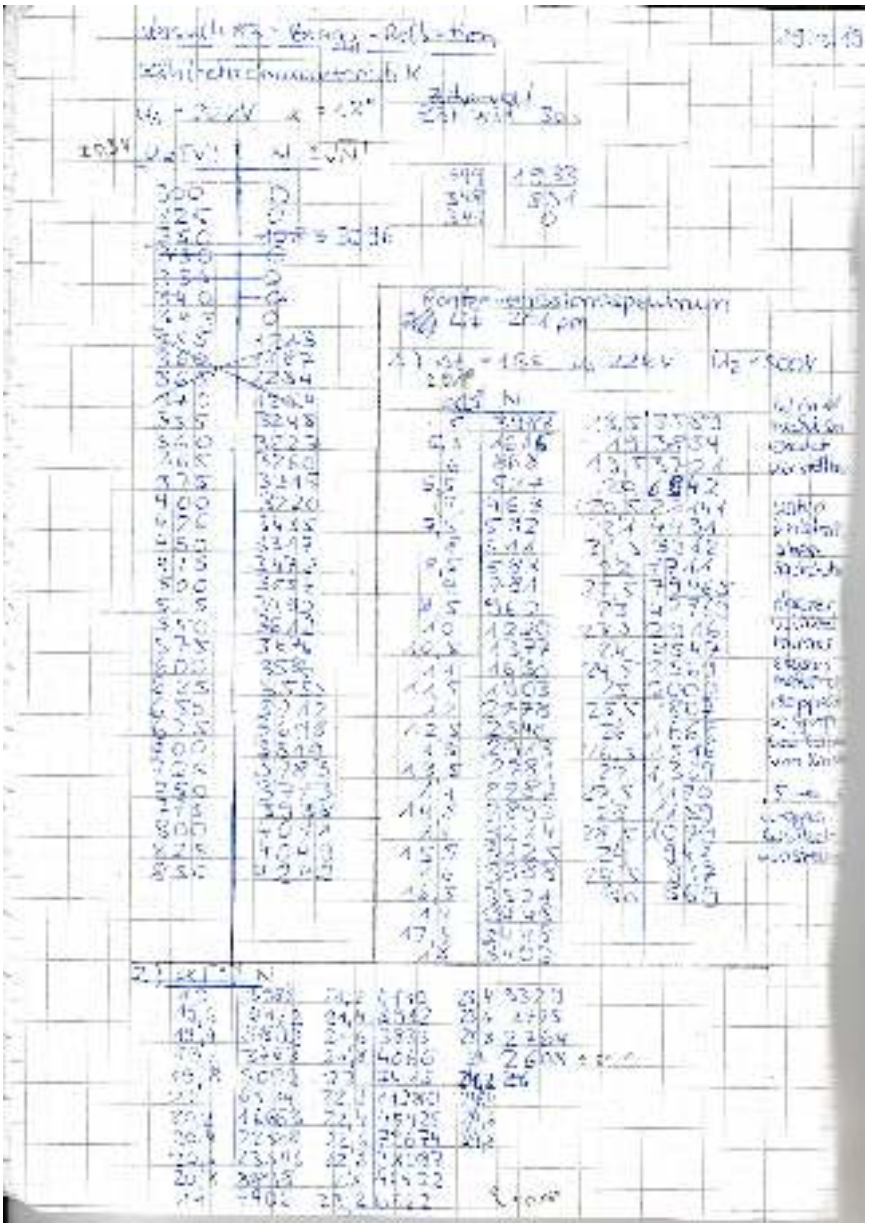

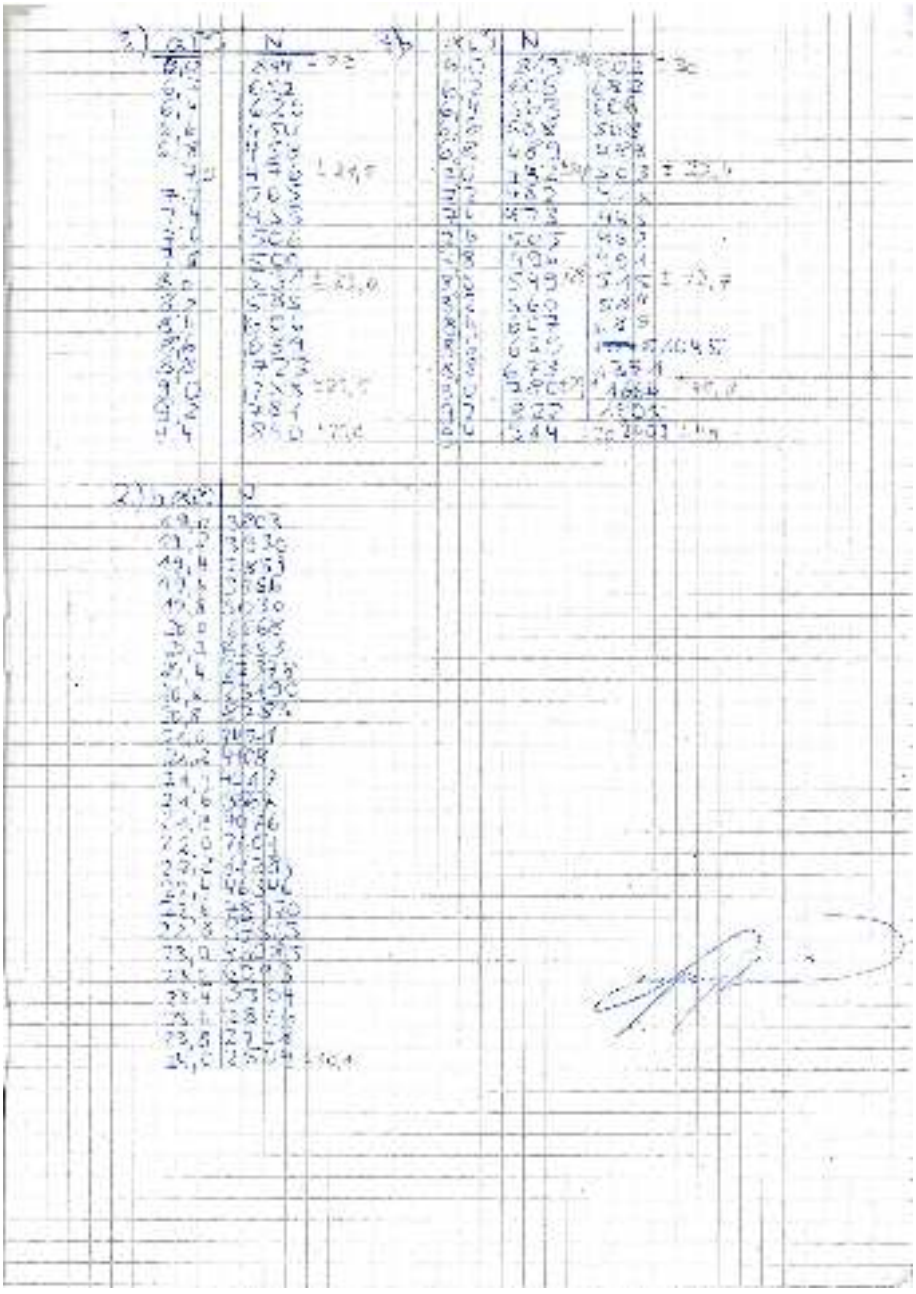

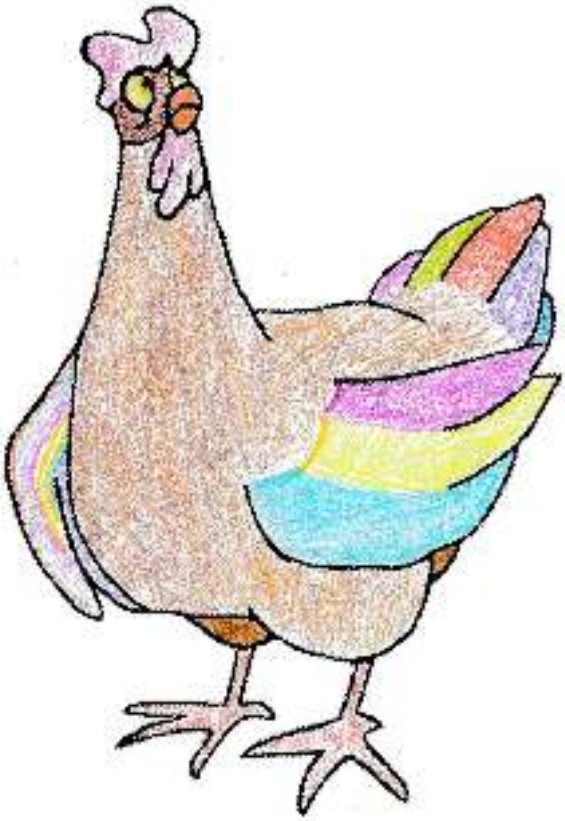

References

[1] Meschede, Dieter: *Gerthsen Physik*. Springer Verlag, 2010. – 1 S.

[2] NIST Physical Measurement Laboratory: *X-Ray Transition Energies*. https://physics.nist.gov/cgi-bin/XrayTrans/search.pl?element=Cu&trans=KM3&lower=&upper=&units=A, 08. June 2009. – [Online; accessed 30. March 2019]

[3] o.V.: *Versuchsanleitungen zum Physiklabor für Anfänger*innen, Teil 2*. 2019